한국기계가공학회지, 제17권, 제6호, pp.46～52(2018.12) ISSN 1598-6721(Print)
Journal of the Korean Society of Manufacturing Process Engineers, Vol. 17, No. 6, pp.46~52(2018.12) ISSN 2288-0771(Online)

https://doi.org/10.14775/ksmpe.2018.17.6.046

Nondestructive Evaluation for Mechanical Degradation of Ultrasuper-Critical Heat-Resistance Steel by Reversible Permeability

SeongBin Ahn*, JaeJin Kim*, DongMin Seo*, ChungSeok Kim*,#

*Department of Materials Science and Engineering, Chosun UNIV.

가역투자율를 이용한 초초임계압 내열강의 기계적 열화에 관한 비파괴평가

안성빈*, 김재진*, 서동민*, 김정석*,#

*조선대학교 재료공학과

(Received 10 September 2018; received in revised form 23 September 2018; accepted 02 October 2018)

ABSTRACT

Nondestructive evaluation for mechanical degradation of ultrasuper-critical (USC) heat-resistance steel, which is attractive to the next generation of power plants is studied by magnetic reversible permeability. The interrelationship between reversible permeability and high-temperature mechanical degradation has been investigated by precise measurement of permeability nondestructively. Also, the effects of microstructural variation on reversible permeability are discussed. Isothermal aging was observed to coarsen the tempered carbides ($Cr_{23}C_6$), generated the intermetallic phases (Fe_2W), and grow rapidly during aging. The dislocation density also decreases steeply within lath interior. The peak to peak interval (PPI) of reversible permeability profile decreased drastically during the initial 500 h aging period, and was thereafter observed to decrease only slightly. The variation in PPI is closely related to the decrease in the number of pinning sites and the degradation in tensile strength.

Key Words : Nondestructive Evaluation(비파괴평가), Permeability(투자율), Ultrasuper-Critical Steel(초초임계압강), Mechanical Degradation(기계적 열화)

1. Introduction

It is necessary to achieve high efficiency represented as high temperature and high pressurization to overcome energy and environmental problems, and the materials used in power generation facilities require high mechanical strength and superior chemical characteristics such as oxidation and corrosion resistance depending on the use conditions. Above all, mechanical strength improvements at high temperature are particularly

Corresponding Author : chs2865@chosun.ac.kr
Tel: +82-62-230-7197, Fax: +82-62-230-7197

important. To improve the thermal efficiency at high temperature and pressure, creep strength and thermal stability higher than those of low chromium ferritic steel, which is the current material widely used in boilers and turbines of ultra-supercritical (USC) power plants. Thus, high chromium ferritic steel has newly been used in boilers and steam turbines in USC power plants and many studies have been actively conducted to improve creep strength and high-temperature safety[1–3]. These types of steel display a tempered martensite lath structure and improve precipitation hardening effects by adding Nb and V and solid-solution hardening effects by adding Cr, Mo, and W.

Material aging occurs where mechanical properties are degraded such as in creep strength and fracture toughness due to diverse and complicated changes in the microstructure when these types of steel are used at high temperature for a long time. Thus, a priori understanding of the microstructure is needed above all to monitor the improvements of reliability and safety of power plants. In addition, many studies on non-destructive evaluation techniques about damage diagnosis of power plants have been conducted[4–8]. In particular, it is well-known that the microstructure such as grain boundary, precipitate, and electric potential plays an important role in the domain wall pinning or domain wall motion in a ferromagnetic body, thereby having a significant effect on magnetic properties. Among the magnetic characteristics, coercive force and Barkhausen noise are changed very sensitively to even minimal changes in the microstructure, so they have been variously applied to studies on material characteristic evaluations.

Ryu et al. reported a correlation with hardness using changes in the mechanical properties of alloy for turbine rotor and coercive force obtained in the first-order harmonic wave, and empirical correlation between reversible permeability and changes in strength have been reported experimentally by measuring the reversible permeability regarding yield strength and tensile strength of steel plates for cars[9, 10].

Although many theoretical and experimental studies have been conducted on the changes in the microstructure of materials using magnetic evaluation method until now, most reports and techniques are nearly impossible to apply in real sites. Thus, we urgently need to develop a non-destructive evaluation technique that can be applied in actual sites and display high defect detection characteristics. This study aims to measure the reversible permeability at the surface of the specimen non-destructively, and through this, measure the coercive force indirectly that is sensitive to changes in material microstructure. We also aim to observe the change in the microstructure according to the high-temperature characteristics of USC ferritic heat-resistant steel, which will be applied to monitor the structural reliability of next-generation power plants.

2. Experiment method

The USC heat-resistant steel used in this study was fabricated through vacuum-induction melting. It was forged at 1100°C followed by normalization treatment for four hours and then tempering treatment at 700°C for 10 hours. The chemical composition of the USC heat-resistant steel is presented in Table 1. An isothermal aging heat treatment was then conducted for up to 8,000 hours at 650°C to evaluate the changes in the microstructure according to aging by accelerating material aging. It was then etched with Vilella's reagent and observed using a scanning electron microscope (SEM) to determine the size and distribution of precipitates and observe the microstructure.

Potentiostatic polarization technique was used for precipitates in the alloy where 3 V was applied to

Table 1 The chemical composition of advanced ferritic 12Cr steel(wt%)

C	Si	Mn	P	S	Ni	Cr
0.19	0.06	0.13	0.013	0.01	0.52	11.01
Mo	W	Co	V	N	Nb	Fe
0.09	3.45	0.21	0.06	0.03	0.01	bal.

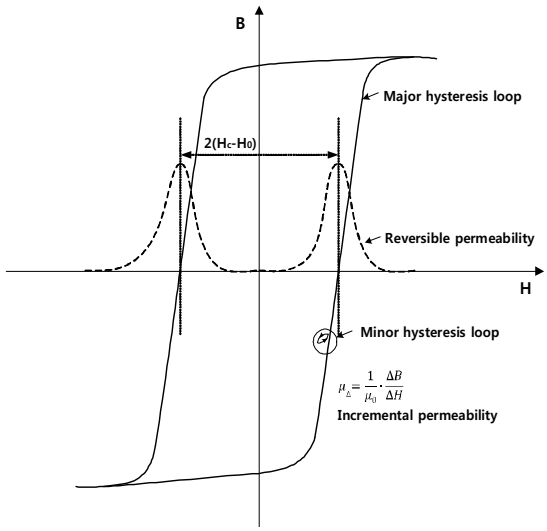

Fig. 1 Hysteresis curve showing the major and minor loops; the dotted line means reversible permeability (μ_r)

the electrolyte extraction solution (100 ml of methanol + 10 m of hydrochloric acid) for 24 hours. The analysis was conducted using Cu Ka with 40 kV and 30 mA up to 30–80°. We observed the dislocation structure and martensite lath using transmission electron microscope (TEM) analysis, and the specimens of the thin film were processed into 3 mm-diameter disks for the analysis, followed by electrolytic polishing at -15°C and 60 V with electrolytes composed of perchloric acid (25%). A search coil, alternating AC perturbation coil, and DC magnetization coil were wound and used by using a ferrite yoke to measure the reversible permeability. The specimens were processed into a plate shape (5 mm-wide, 30 mm-long, and 1 mm-thick). For magnetization, and the maximum magnetic field was 12 kA/m by applying a 0.05 Hz sine wave, and 80 A/m and 40 Hz were added via a perturbation magnetic field. Fig. 1 shows the typical magnetization curve that displays the relationship between the magnetic flux density (B) and magnetic field (H). In particular, when an AC magnetic field was applied to DC magnetic field, the major hysteresis loop changed along the minor hysteresis loop. The infinitesimal change rate of the applied magnetic field with regard to the magnetic flux density is called the incremental permeability and the permeability when the infinitesimal change in the applied magnetic field converges to zero is called the reversible permeability. Fig. 1 shows the profile of the reversible permeability obtained by the derivative in the magnetic hysteresis curve. The two peaks in the profile of the reversible permeability are symmetrical, and the maximum peak-to-peak interval (PPI) is equivalent to 2 (Hc + Ho). Here, Hc refers to the dynamic coercivity, and Ho refers to the size of the modulated magnetic field, which has a much smaller value than the size of the applied magnetic field. Thus, the PPI is twice the size of the dynamic coercivity in general.

3. Experiment results and discussion

Fig. 2 shows the microstructure observed after tempering and aging up to 8,000 hours. The microstructure after tempering showed a total tempered martensite structure as shown in Fig. 1(a), and the mean size of the crystal grain was approximately 100 μm. In addition to the prior austenite (PAG) boundary and packet boundary, the martensite lath had an approximate width of 0.2 μm. Somewhat coarse precipitates in the austenite boundary and precipitates extended in the arranged direction of trans-granular lath were present. Only

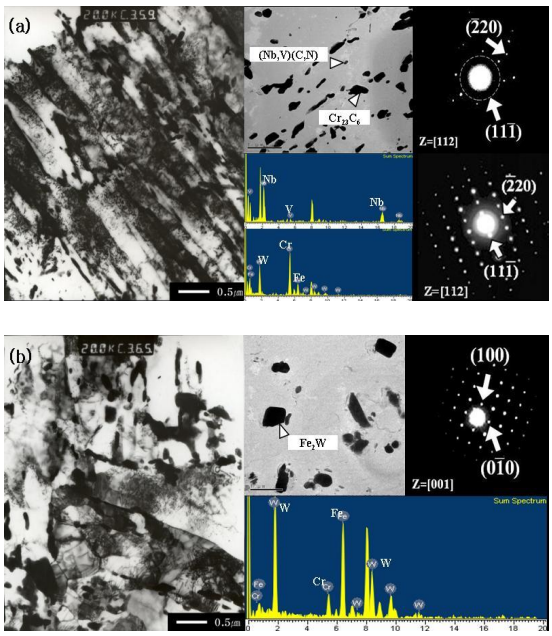

Fig. 2 Micrographs of ultra super-critical steel subjected to tempering and 8000h aging showing TEM image, carbon replication of tempered specimen: (a) as-tempered and (b) 8000h aging specimen

the precipitates were replicated from the base metal using a carbon extraction replica method and observed by the TEM to analyze the precipitates. The presence of coarse Cr23C6 precipitates and MX phase such as minute spherical NbC or VC was observed in the grain. The minute precipitates observed in this study were (V,Nb) and (N,C), which were too small at approximately 20–50 nm, and the size change was minimal according to the material aging. Most precipitates were coarsened as the aging time increased. In particular, the coarsening of the grain boundary precipitates progressed rapidly. The size of the precipitates increased in proportion with the aging time and the number of precipitates per unit area was reduced. The coarsening of the precipitates was due to the

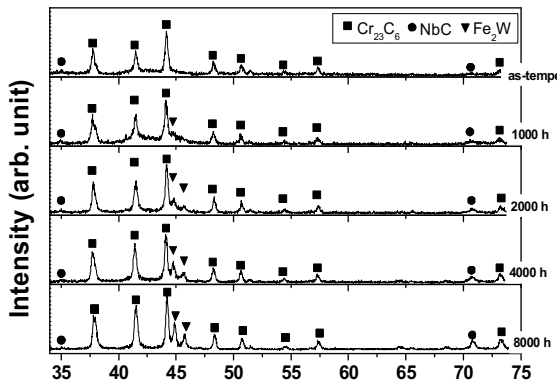

Fig. 3 XRD profiles of ultra super-critical steel subjected to material degradation showing variation in secondary phases

Ostwald growth, in which growth occurred while the interfacial energy between the precipitate and base metal reduced according to the diffusion mechanism. Since it can reduce the effects of precipitation and solid-solution hardening, it can cause a significant reduction in the impact energy as reported in a previous study[5].

Fig. 1(b) shows the TEM photo after 8,000 hours of aging. The lath width of the martensite was increased significantly and had grown considerably from 0.2 μm prior to processing to 0.6 μm after thermal treatment. The size of the precipitate also grew significantly. According to the Ostwald coarsening theory, the number of precipitates per unit area was also significantly reduced. The highly coarse and newly generated Fe2W precipitates were observed as shown in the photo of the carbon extraction replica and diffraction pattern analysis showed a hexagonal crystal structure. The electron diffraction pattern in the image observed in the thin-film specimen was aged for 8,000 hours and tempering showed a typical precipitate over the material-aging time. The early specimen after tempering showed a typical lath structure of tempered martensite whose dislocation density was

significantly high. Several-to-dozens of the nano-sizes of fine NbC and VC phases were distributed inside the lath and Cr23C6 was evenly distributed in both the lath and PAG boundaries.

The early fine Cr23C6 phase became coarsened as aging progressed and compounds between the new metals around the lath were precipitated. These precipitates were known as Laves phases through TEM analysis. In particular, Laves phases showed a rapid coarsening rate according to their aging. The dislocation density inside the lath was also rapidly reduced as the aging progressed. Fig. 3 shows the X-ray diffraction analysis results on the precipitate particle powders after selectively extracting just the precipitate phase. Only the diffraction peak that displayed Cr23C6 and NbC phases was observed for the tempered specimen prior to early aging.

However, the diffraction peak of Fe2W was revealed as the aging time increased, which further increased the diffraction strength due to the increase in aging time. Thus, this was due to the increase in the fraction of the Fe2W phase as observed in the TEM in Fig. 2. Fig. 4 shows the typical reversible permeability profile that displays the changes in reversible permeability with regard to the applied magnetic field measured for each aged specimen. The maximum peak of the reversible permeability is a characteristic displayed during the magnetization process of a ferromagnetic body, which exhibited that the location of the maximum peak was decreased as the aging hours increased.

The change in the PPI is shown in Fig. 5(b). The PPI of the reversible permeability was rapidly decreased within about 500 hours, which was then followed by slight but monotonous reduction. In addition, the reduction in mechanical strength was the typical physical phenomenon due to high-temperature aging (isothermal tempering, creep, and fatigue). In this study, hardness and tensile strength were reduced as the high temperature and aging time increased. The change in strength was

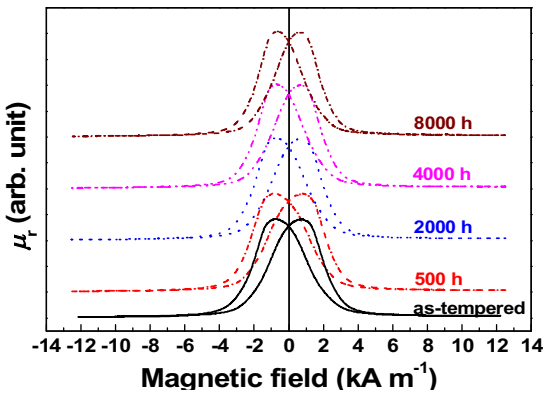

Fig. 4 Reversible permeability (μr) profiles of ultra super-critical steel subjected to material

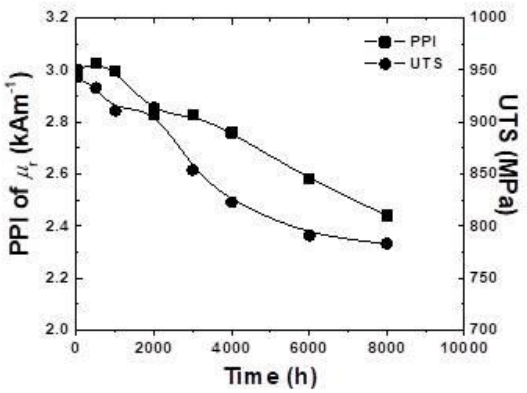

Fig. 5 Peak to peak interval of reversible permeability and ultimate tensile strength of ultra super-critical steel subjected to material degradation

closely related to the change in the PPI of the reversible permeability. The change in the PPI of the reversible permeability according to material aging was reduced with the increase in aging hours as shown in Fig. 5(b). As described above, coercive force (Hc) was the maximum resistance against domain wall motion in physical ferromagnetic materials, and non-magnetic inclusions, dislocation, and grain boundary are some of the major obstacles to domain wall motion in ferromagnetic materials[11].

Non-magnetic inclusions are generally reportedly proportional to the volume fraction of the inclusion in the relationship with coercive force. Inclusions differ in their effect on the coercive force depending on the thickness and relative size of the domain wall; thus, size dependence should be considered.

However, since most precipitates are larger than the thickness of the domain wall (approximately 30 nm for iron)[9] immediately after tempering and as aging progresses, the domain wall motion is obstructed by forming spike magnetic domain structures. In particular, the effect of precipitates with a similar size to the domain wall thickness is most significant. In this regard, precipitates that affect the magnetic properties of USC heat-resistant steel are fine MX precipitates. However, they are excessively stable, so transformation, re-dissolution, and coarseness are rare occurrences. Thus, although they may affect the magnetic properties, the effect according to the aging level can be ignorable. Furthermore, precipitates have been known to contribute significantly to the strength as they obstruct the dislocation mobility. However, such a precipitation hardening effect cannot be achieved if non-coherency occurs in contrast with the case that forms the coherent strain as the precipitates and base metal have a coherent relationship. Moreover, the cut and move mechanism of precipitates is no longer effective upon dislocation moving with precipitate coarsening, and the particle loop mechanism is effective according to the Orowan and Ashby[12] model, thereby reducing the strength as the size of precipitates increases. Therefore, the precipitate-coarsening results in less coherence between the precipitate and base metal, ultimately leading to strength reduction.

The dislocation also creates local micro-stresses inside materials, thereby forming a strain field that disturbs the domain wall motion. The reduced dislocation density and precipitate coarsening cause the recovery of the lath structure, which is a strong strengthening mechanism in ferritic USC heat-resistant steel. The lath martensite consists of diverse and structurally complicated boundaries. However, only the lath boundary grew significantly; no changes in the boundaries were revealed even though aging progressed in the material aging process in this study. The role of the lath that contributed to the strength was analyzed as being similar to that of the crystal grain as the lath was considered to reduce the crystal grain while having a similar physical role. The lath boundary is thought to have a significant effect on the domain wall motion as magnetic moment deflection occurs at the ground boundary as the same time as the existing crystal grains. However, few studies have been conducted on whether the role of the martensite lath in the domain wall motion is similar to that of the crystal grains. Thus, more in-depth and systematic studies are needed on the above matter in the future.

4. Conclusions

This study evaluated the microstructural change in USC heat-resistant steel according to high-temperature material aging by measuring the reversible permeability and obtained the following conclusions.

1. The non-destructive measurement of reversible permeability was achieved successfully using a yoked probe at the surface of the specimens.
2. Fine Cr23C6 precipitates grew at early tempering in the heat-resistant steel due to high-temperature material aging, and compounds between the new Fe2W metals were generated, thereby showing rapid coarsening.
3. The lath boundary, which was pinned by the precipitates prior to aging due to the precipitate coarsening, was moved and integrated, resulting in increased lath width. Thus, the tensile strength was reduced.

4. This study found that reversible permeability was closely related to the reduction in the number of precipitates, dislocation density, and increased lath width. Conclusively, the non-destructive measurement using reversible permeability can monitor the material aging process of USC heat-resistant steel.

Acknowledgment

This study was supported by the Sprout Research Talent Support Program for 2017 Undergraduate Students by Chosun University (Undergraduate Scholarship Program).

REFERENCES

1. Abe, F., “Bainitic and Martensitic Creep-Resistant Steels,” Current Opinion in Solid State and Materials Science, Vol. 8, No. 3, pp. 305-311, 2004.
2. Kim, C. S., “A Study of the Heat Treatment Effect on the Fatigue Crack Growth Low-Carbon Steel and AISI316 Authentic Stainless Steel,” Journal of the Korean Society of Manufacturing Process Engineers, Vol. 17, No. 3, pp. 16-21, 2018.
3. Kimura, M., Yamaguchi, K., Hayakawa, M., Kobayashi, K., Kanazawa, K., “Microstructures of Creep-fatigued 9-12% Cr Ferritic Heat-resisting Steels,” International Journal of Fatigue, Vol. 28, No. 3, pp. 300-308, 2006.
4. Kim, C. S., Park, I. K., Jhang, K. Y., “Nonlinear ultrasonic characterization of thermal degradation in ferritic 2.25Cr-1Mo steel,” NDT & E Int.ernational Vol. 42, No. 3, pp. 204-209, 2009.
5. Luxenburger, S., Arnold, W., “Laser ultrasonic absorption measurement in fatigue-damaged materials,” Ultrasonics, Vol. 40, No. 1-8, pp. 797-801, 2002.
6. Dobmann, G., Kroning, M., Theiner, W., Willems, H., Fiedler, U., “Nondestructive characterization of materials (ultrasonic and micromagnetic techniques) for strength and toughness prediction and the detection of early creep damage,” Nuclear Engineering Design, Vol. 157, No. 1-2, pp. 137-158, 1995.
7. Gupta, S., Ray, A., Keller, E., “Online fatigue damage monitoring by ultrasonic measurements: A symbolic dynamics approach,” International Journal of Fatigue, Vol. 29, No. 6, pp. 1100-1114, 2007.
8. Kim, C. S., Kwun, S. I., “Influence of Precipitate and Martensite Lath on the Magnetic Properties in Creep Damaged 11Cr-3.45W Steel,” Journal of Materials Transactions, Vol. 48, No. 11, pp. 3028-3030, 2007.
9. Ryu, K. S., Nahm, S. H., Park, J. S., Yu, K. M., Kim, Y. B., Son, D. R., “Nondestructive evaluation of aged 1Cr-1Mo-0.25 V steel by harmonic analysis of induced voltage,” Journal of magnetism and magnetic material, Vol. 231, No. 2-3, pp. 294-298, 2001.
10. Ryu, K. S., Kim, Y. I., Nahm, S. H., Yu, K. M., Cho, Y., Son, D. R., “Degradation Evaluation of 1Cr-lMo-0.25V Steel by Measuring Reversible Magnetic Permeability,” Journal of the Korean Society for Nondestructive Testing, Vol. 20, No. 5, pp. 445-450, 2000.
11. Cullity, B. D., Introduction to Magnetic Materials, Reading, Mass., Addison-Wesley Pub. Co., 1972.
12. Verhoeven, J. D., Fundamentals of Physical Metallurgy, John Wiley & Sons, New Yrok, USA, 1975.